Bull. Mater. Sci., Vol. 9, No. 4, November 1987, pp. 269–275. © Printed in India.

Kinetics of crystallization of a $Fe_{74}Co_{10}B_{16}$ glass

R P MATHUR and D AKHTAR
Defence Metallurgical Research Laboratory, Hyderabad 500 258, India

MS received 29 June 1987

Abstract. Differential scanning calorimetry (DSC) technique has been employed to study the crystallization kinetics of a $Fe_{74}Co_{10}B_{16}$ glass. Crystallization of $Fe_{74}Co_{10}B_{16}$ glass is known to occur in two distinct stages. It was possible to separate out the isothermal kinetics of both the crystallization stages through a thermal treatment scheme in the DSC. The crystallization processes are interpreted in the light of the kinetic data obtained.

Keywords. Metallic glass; crystallization; incubation time; activation energy; Avrami exponent.

1. Introduction

Continuous heating of $Fe_{74}Co_{10}B_{16}$ glass in a differential scanning calorimeter (DSC) exhibits two exothermic events (Akhtar *et al* 1986) which are separated by a temperature interval of 84 K at a heating rate of 20 K/min. It has been shown (Mathur *et al* 1987) that the first event corresponds to the precipitation of α-Fe from the amorphous matrix and the second event corresponds to the crystallization of the remaining amorphous phase into Fe_3B and Co_2B phases.

In the present study, isothermal kinetics of both the crystallization events of $Fe_{74}Co_{10}B_{16}$ glass have been investigated using the DSC technique. A thermal treatment scheme in the DSC comprising isothermal anneals at two temperatures, given to the same specimen (Akhtar 1986), was employed. The crystallization processes are interpreted in the light of the kinetic data obtained.

2. Experimental

Details of the preparation of $Fe_{74}Co_{10}B_{16}$ glass ribbons are given elsewhere (Akhtar *et al* 1986; Mathur *et al* 1987). DSC experiments were carried out in an advanced thermal analysis system, the computerized DuPont 1090. This instrument allowed a good control over the temperatures of isothermal scans. It heats up to the temperature set for isothermal scan at the maximum possible heating rate. Typically, a temperature of 500°C could be arrived at in 3–4 min starting from room temperature. The data could be stored, processed and compared, thus making it simple to produce plots for accurate comparison.

3. Results and discussion

Typical continuous heating DSC thermogram obtained at a heating rate of 20 K/min is shown in figure 1a. The two exothermic peaks observed in the DSC thermogram reveal two stages of crystallization of the $Fe_{74}Co_{10}B_{16}$ glass as discussed earlier. To determine the kinetics of the crystallization processes, a two-step isothermal

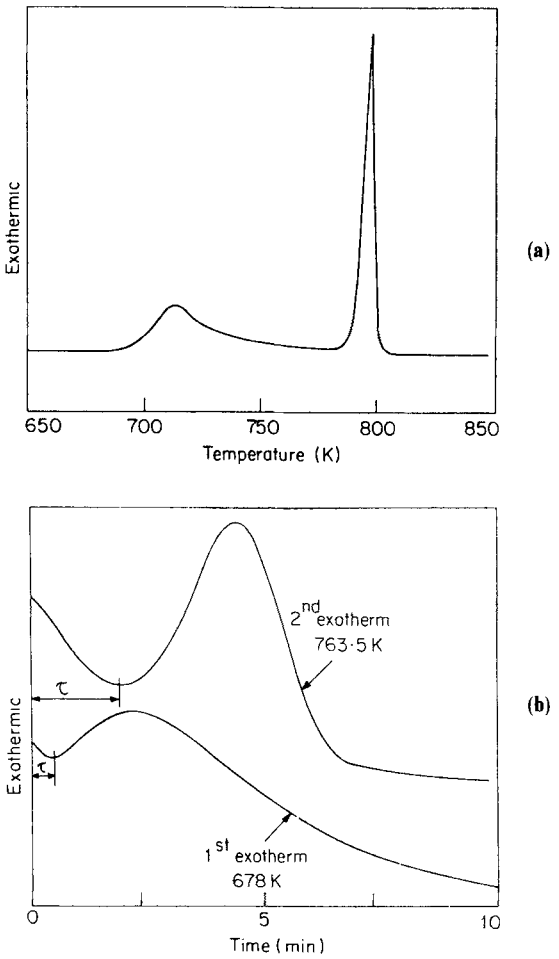

Figure 1. **a.** Crystallization exotherms obtained at a heating rate of 20 K/min. **b.** Typical isothermal exotherms depicting the incubation period, τ.

treatment was devised. The first isothermal anneals were carried out in the temperature range 678 K to 685 K. Anneals at higher temperatures could not be carried out because of the normally encountered difficulty of the incubation time falling short of the instrument transient time. At temperatures lower than 678 K, because of slow transformation rates, the exotherm tended to flatten out. In the temperature range of investigation, the base line became linear after the end of the instrument transient and a well-defined isothermal exotherm could be obtained. After completion of the first stage of crystallization, the base line in the isothermal thermogram became parallel to the time axis indicating an undetectable rate of exothermic reaction.

The second crystallization event did not occur at a detectable rate at the first annealing temperatures. Thus it was necessary to heat the specimen rapidly to the temperatures of second isothermal anneals in order to study the isothermal kinetics of the second event. The second anneals were performed in the temperature range 763·5 K to 772·5 K, the upper and lower temperature limits being again governed by

the factors described above. Observation of a well-defined incubation period for the second anneal suggested that (i) the formation of α-phase was complete before the second annealing temperature was arrived at and (ii) during the heating-up period between the two annealing treatments, the second crystallization event did not start. Operation of either of these processes would have caused the disappearance of the incubation period.

The incubation period was taken as the time interval between the specimen reaching the annealing temperature and the start of the transformation. The start of the transformation was taken as that instant at which the base line first deviated from linearity. Typical isothermal exotherms depicting the incubation period, τ for both the stages of crystallization are shown in figure 1b. The incubation times observed at some annealing temperatures are listed in table 1 for both the crystallization events. The observed decrease in the incubation period with increasing annealing temperature was in keeping with the fact that at temperatures below the nose of the time - temperature-transformation curve for crystallization, the nucleation rate increases with increasing temperature, resulting in a decrease in the incubation period (Scott and Ramachandrarao 1977).

The kinetics of the two crystallization processes were analysed in terms of the following expression of the generalized theory of phase transformations (Burke 1965)

$$x = 1 - \exp(-bt^n),$$

where x is the fraction transformed in time t, b is a rate constant and n the Avrami exponent. The fraction transformed x at any time t was determined as the ratio $A(t)/A(\text{tot})$ where $A(t)$ and $A(\text{tot})$ are the area under the isothermal exotherm up to time t and the total area of the exotherm respectively. Plots of x vs time at different temperatures yielded sigmoidal curves, shown in figures 2a and 2b for the first and second crystallization events respectively.

The activation energy of the crystallization processes was evaluated from the isothermal exotherms making use of the Arrhenius relation

$$t_x = t_0 \exp(E/RT),$$

where t_x is the time required for the transformation of fraction x at temperature T and E is the activation energy. The plots of t_x ($x = 0{\cdot}3$, $0{\cdot}5$ and $0{\cdot}8$) against $1/T$ are shown in figures 3a and 3b for the first and second stages of crystallization respectively. Calculated values of activation energy are depicted in the figures. The Avrami exponent n was determined by evaluating the slope of the plots of $\ln[-\ln(1-x)]$ against $\ln t$. Such plots are shown in figures 4a and 4b for the first and second cry-

Table 1. Values of incubation times at some annealing temperatures.

I stage		II stage	
Temperature (K)	Incubation time (min)	Temperature (K)	Incubation time (min)
678	0·35	763·5	1·8
682·5	0·25	767	0·65
685	0·2	768	0·5
		772·5	0·3

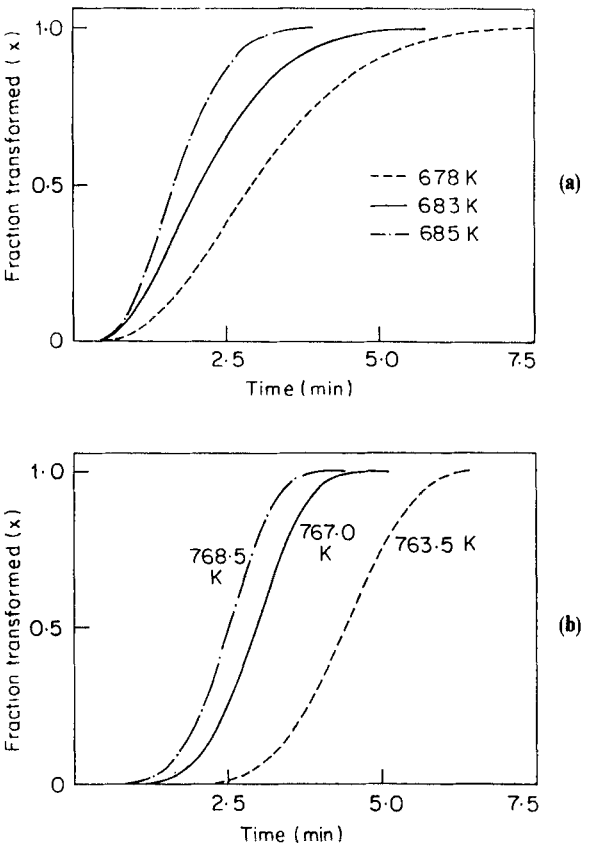

Figure 2. Some of the sigmoidal curves for **a.** first crystallization stage and **b.** second crystallization stage.

stallization events respectively. Estimated values of the Avrami exponent are also depicted in the figures.

The crystallization kinetics of iron-based metallic glasses containing boron have been studied by various investigators (Greer 1982; Chang and Marti 1983; Baburaj *et al* 1985; Miranda *et al* 1986a, b), particularly because of the favourable properties of these glasses. Activation energy values ranging from 2·4–2·5 eV (Greer 1982; Baburaj *et al* 1985) to 3·7–3·8 eV (Chang and Marti 1983; Akhtar 1986) have been obtained for the precipitation of α-Fe phase. Our activation energy of 3·2–3·3 eV for the first stage of crystallization of $Fe_{74}Co_{10}B_{16}$ glass lies within the range of reported values. Activation energies of 4·8 and 5·2 eV reported by other investigators (Miranda *et al* 1986a, b), however, appear to be too high for the primary crystallization process. A comparison of activation energies for the second crystallization event would not be proper since the structure/composition of the phase(s) corresponding to this stage is not similar. In $Fe_{74}Co_{10}B_{16}$ glass, Fe_3B and Co_2B phases are formed simultaneously in the second stage which requires an average activation energy of 5·2–5·7 eV. The effective activation energy of crystallization is determined by both nucleation and growth processes. It is therefore not possible to attach any physical significance to the values of the activation energies. It is noteworthy that the activation energy

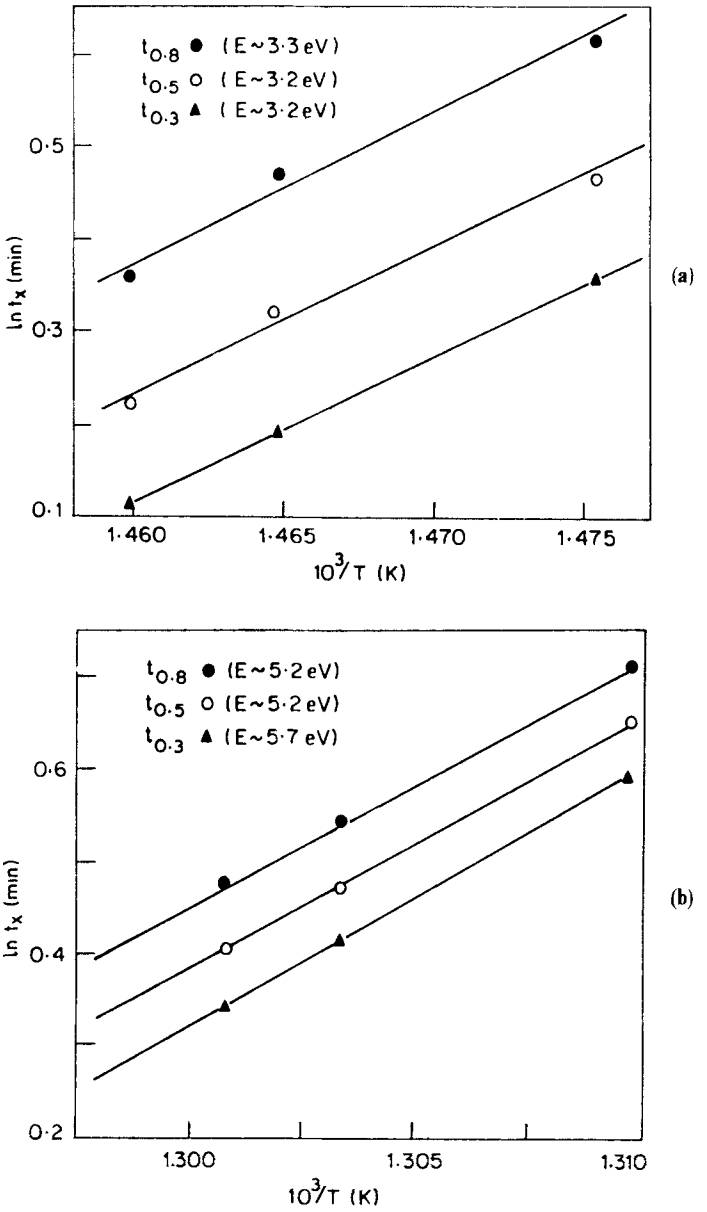

Figure 3. Plots of $\ln t_x$ against $1/T$ for **a.** first crystallization stage and **b.** second crystallization stage.

values are much larger than those expected for simple diffusive processes and may be taken as an indication of the complexity of the crystallization kinetics on which such factors as diffusion, nucleation mechanisms and interface processes may exert an influence.

For the primary crystallization process, the value of the Avrami exponent $n = 2{\cdot}2$ estimated in the present investigation is slightly lower than the value of 2·5 obtained for Metglas 2605 SC (Akhtar 1986) but higher than the values of 2·0 and 1·7 obtained

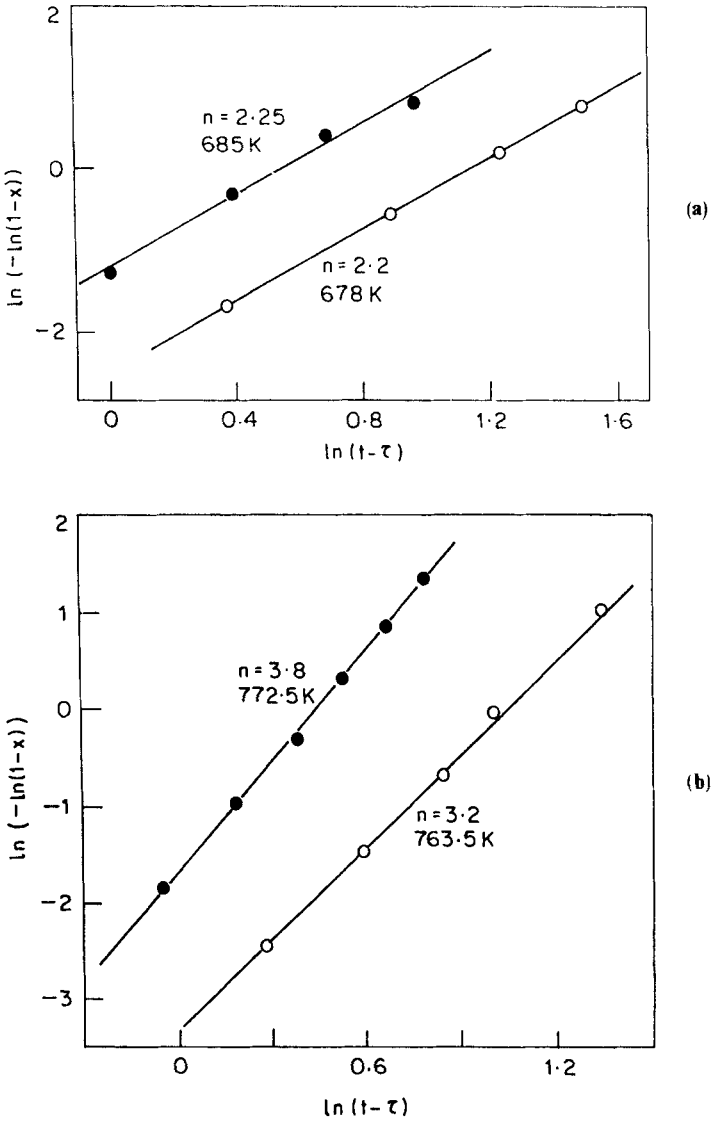

Figure 4. Plots of $\ln[-\ln(1-x)]$ against $\ln(t-\tau)$ for **a.** first crystallization stage and **b.** second crystallization stage.

for primary crystallization of Metglas 2605 CO (Baburaj *et al* 1985) and Metglas 2826A (Von Heimendahl and Kuglstatter 1981). Let us consider the expression for n (Christian 1975)

$$n = a + pd,$$

where $p = 1$ for linear growth, $p = 1/2$ for parabolic growth; $d = 1$, 2 or 3 for one; two- or three-dimensional growth; $a = 0$ for no nucleation (i.e. zero nucleation rate), $a = 1$ for constant nucleation rate, $0 < a < 1$ for a decreasing nucleation rate and $a > 1$ for an increasing nucleation rate. Our n value of 2·2 for the primary crystallization of $Fe_{74}Co_{10}B_{16}$ glass is thus indicative of a process involving nucleation at a decreasing

rate with time and a parabolic growth. For the second crystallization stage, the values of n obtained in the present investigation vary from 3·2 to 3·8. A direct interpretation of these values is not possible because these Avrami exponents correspond to the formation of both Fe_3B and Co_2B phases in the second stage. Nevertheless, they imply a nucleation rate which decreases with time and a linear growth process.

4. Conclusions

It was possible to separate out the isothermal kinetics of both the crystallization stages of $Fe_{74}Co_{10}B_{16}$ glass. The kinetic data thus obtained imply a decreasing nucleation rate (with time) and a parabolic growth for the first crystallization stage and a decreasing nucleation rate (with time) and a linear growth process for the second crystallization stage.

Acknowledgements

Thanks are due to Mr V N Murthy and Dr P Subrahmaniam for their help in preparation of the alloy.

References

Akhtar D 1986 *Scr. Metall.* **20** 983
Akhtar D, Murthy V N, Subrahmaniam P and Jagannathan R 1986 *J. Mater. Sci. Lett.* **5** 1148
Baburaj E G, Dey G K, Patni M J and Krishnan R 1985 *Scr. Metall.* **19** 305
Burke J 1965 *Kinetics of phase transformation in metals* (Oxford: Pergamon Press)
Chang C F and Marti J 1983 *J. Mater. Sci.* **18** 2297
Christian J W 1975 *The theory of phase transformation in metals and alloys*' (Oxford: Pergamon Press)
Greer A L 1982 *Acta Metall.* **30** 171
Mathur R P, Murthy V N, Akhtar D, Subrahmaniam P and Jagannathan R 1987 *J. Mater. Sci. Lett.* **6** (in press)
Miranda H, Conde C, Conde A and Marquez R 1986a *Mater. Lett.* **4** 226
Miranda H, Conde C, Conde A and Marquez R 1986b *Mater. Lett.* **4** 442
Scott M G and Ramachandrarao P 1977 *Mater. Sci. Eng.* **29** 137
Von Heimendahl M and Kuglstatter G 1981 *J. Mater. Sci.* **16** 2405